The Physics of Chromospheric Plasmas
ASP Conference Series, Vol. 368, 2007
Petr Heinzel, Ivan Dorotovič and Robert J. Rutten, eds.

arXiv:astro-ph/0611488v2 1 Apr 2007

Spectral Diagnostics of Active Prominences

Nicolas Labrosse[1], Pierre Gouttebroze[2] and Jean-Claude Vial[2]

[1]*Institute of Mathematical and Physical Sciences, Aberystwyth, UK*
[2]*Institut d'Astrophysique Spatiale, Orsay, FR*

Abstract. Active prominences exhibit plasma motions, resulting in difficulties with the interpretation of spectroscopic observations. These solar features being strongly influenced by the radiation coming from the solar disk, Doppler dimming or brightening effects may arise, depending on which lines are observed and on the velocity of the plasma. Interlocking between the different atomic energy levels and non local thermodynamic equilibrium lead to non-trivial spectral line profiles, and this calls for complex numerical modeling of the radiative transfer in order to understand the observations. We present such a tool, which solves the radiative transfer and statistical equilibrium for H, He I, He II, and Ca II in moving prominences where radial plasma motions are taking place. It is found that for isothermal, isobaric prominence models, the He II resonance lines are very sensitive to the Doppler effect and thus show a strong Doppler dimming. The Ca II lines Doppler effect for the prominence models considered here. We illustrate how the code makes it possible to retrieve the plasma thermodynamic parameters by comparing computed and observed line profiles of hydrogen and helium resonance lines in a quiescent prominence. This new non-LTE radiative transfer code including velocities allows us to better understand the formation of several lines of importance in prominences, and in conjunction with observations, infer the prominence plasma thermodynamic properties and full velocity vector.

1. Introduction

The main motivation of our modeling work is to contribute to building realistic prominence models. For this, we need an accurate knowledge of thermodynamic quantities (temperature, densities, ...), level populations (useful, e.g., to infer the magnetic field properties from spectro-polarimetric observations), velocity fields, energy budget. However these quantities still have large uncertainties associated with them. Observations of several different lines from different atoms/ions allow us in theory to measure these parameters. Among these lines, the H and He lines are important as they are strong and largely contribute to the radiative losses. However the prominence plasma being out of LTE and optically thick in H and He resonance lines, the interpretation of line spectra or intensities in radially moving prominences is a non-trivial task. Therefore, non-LTE radiative transfer calculations including velocity fields are needed to build realistic prominence models. Here we present such calculations and preliminary results.

2. Modeling Procedure

The prominence is represented by a 1D plane-parallel slab standing vertically above the solar surface. Each prominence model is defined by a set of free parameters: the temperature T, the gas pressure p, the slab thickness L (or the total column mass), the height of the slab above the limb H, the microturbulent velocity, and the radial speed. For this preliminary study we consider isothermal and isobaric prominences, although the code allows for inclusion of a transition region between the cold prominence and the hot corona. We first solve the pressure equilibrium, the ionization equilibrium, and the coupled statistical equilibrium (SE) and radiative transfer (RT) equations for a 20 levels H atom. Then the SE and RT equations are solved for other elements: He I (29 levels) and He II (4 levels), and Ca II (5 levels). More details on the modeling of the hydrogen, calcium, and helium spectra in quiescent prominences can be found in Gouttebroze & Labrosse (2000); Gouttebroze & Heinzel (2002); Labrosse & Gouttebroze (2004) respectively, and references therein.

For the modeling of active and eruptive prominences, we use a velocity-dependent incident radiation as boundary conditions for the RT equations. It has already been shown by Heinzel & Rompolt (1987) in the case of the hydrogen lines that the Doppler effect induces a frequency shift of the incident profile relative to the rest case, and also a distortion of the incident profile due to the variation of the Doppler shift with the direction of the incident radiation. It is also the case for the helium (Labrosse et al. 2006) and calcium incident radiation.

3. Diagnostics of Radial Velocities

3.1. Integrated intensities

We reproduce the results of Gontikakis et al. (1997a,b) who computed the hydrogen radiation emitted by a radially moving prominence, using partial redistribution in frequency (PRD) for the Lyman lines. We obtain the same variation of the relative intensities (intensities normalised to the line intensities when the prominence is at rest) and the same line profiles for Lyα, Lyβ, and Hα. The main result is that there exists an important coupling between Lyβ and Hα which causes these lines to be first Doppler brightened, and then Doppler dimmed, with increasing velocity, while there is only a Doppler dimming effect on Lyα.

Figure 1 presents relative intensities as a function of velocity for the He I 584 Å, He II 304 Å, and He I 10830 Å lines (left panel) and Ca II K and Ca II 8542 Å lines (right panel) at two different temperatures (8000 K and 15000 K).

The He I 10830 Å line does not show any sensitivity to the Doppler effect, which is mainly due to the very weak incident absorption line. The He I 584 Å line is quite sensitive to the Doppler effect. Its Doppler dimming is more important at low temperature. The He II resonance lines are the most sensitive to the radial velocity of the plasma (the relative intensity of the He II 256 Å line, not shown, exhibits a similar variation as He II 304 Å), and the Doppler dimming is strong at the temperatures considered in this study. Such a result was expected

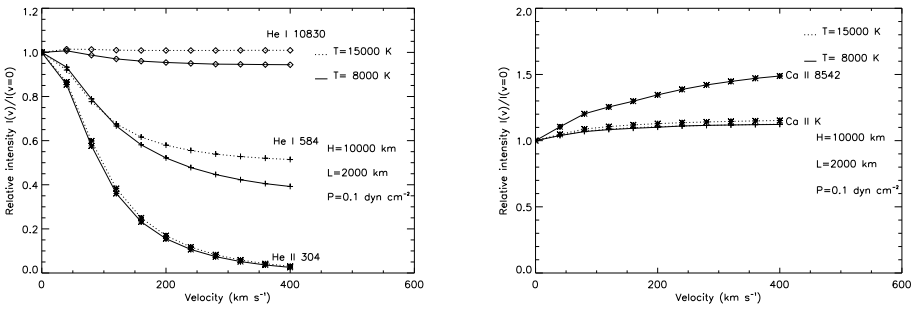

Figure 1. Relative intensities (intensities normalized to the line intensity at rest) as a function of velocity at 8000 K (solid lines) and 15000 K (dotted lines) for left: He I 10830 Å (diamonds), He I 584 Å (plus), and He II 304 Å (stars); right: Ca II K (plus) and Ca II 8542 Å (stars).

since the main mechanism of formation at these temperatures for these lines is the scattering of the incident radiation (Labrosse & Gouttebroze 2001). Let us stress that in this preliminary study we have not included a transition region between the cold prominence and the hot corona (PCTR). The presence of a hotter plasma in the PCTR may somehow decrease the sensitivity of the He II resonance lines to the Doppler effect as collisions will become more important in the formation processes of these lines. This will be investigated in a future work.

The right panel of Fig. 1 indicates that there is no strong Doppler effect on the Ca II resonance lines, while we observe some Doppler brightening of the 8542 Å line (and indeed of the other two infrared lines at 8498 and 8662 Å, not shown) at low temperature.

3.2. Line profiles

If spectroscopic observations of erupting prominences are available, then a comparison between computed and observed line profiles can be made. We show in Figs. 2 and 3 the line profiles for the same helium and calcium lines considered in Fig. 1 at two different temperatures (solid line: 8000 K, dashed line: 15000 K), at four different velocities (from top to bottom: 0, 80, 200, and 400 km s^{-1}).

The Doppler dimming effect is well observed in the helium resonance lines at 584 Å and 304 Å as the radial velocity is increased (Fig. 2). We can observe asymmetries in the line profiles of these lines when the prominence plasma is moving radially, with some intensity enhancement which is especially visible in the red wing of the He I 584 Å line at low temperature. This is explained as follows. The radiation emitted by the disk center in our code is represented by symmetrical line profiles. When the prominence is at rest, the incident radiation illuminating the prominence slab is symmetrical; however when the prominence plasma is moving radially the incident line profile becomes distorted and shifted towards the red. As we used the PRD standard approximation in our calculations of the resonance lines of helium, the resulting line profiles are asymmetrical. This would not have been the case if we had considered complete redistribution in frequency (CRD) instead of PRD. The line asymmetry is more visible for

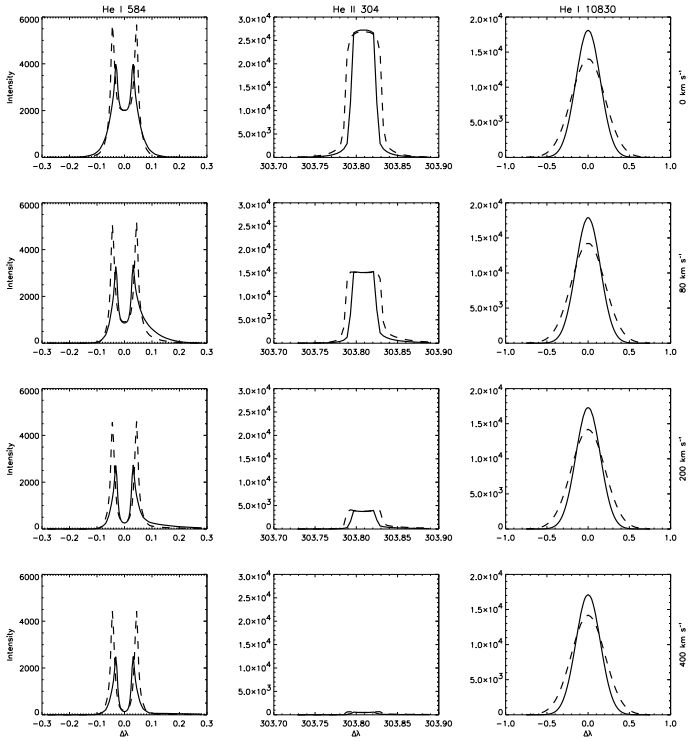

Figure 2. Line profiles for $T = 8000\,\mathrm{K}$ (solid line) and $T = 15\,000\,\mathrm{K}$ (dashed line), with $p = 0.1$ dyn cm^{-2}, and $L = 2000$ km, at different velocities: 0, 80, 200, and 400 km s^{-1} from top to bottom. Abscissa is $\Delta\lambda$ in Å and vertical axis is specific intensity in erg s^{-1} cm^{-2} sr^{-1} Å^{-1}. From left to right: He I 584 Å, He II 304 Å, and He I 10830 Å.

the He I 584 Å line as its wings are fairly bright, while the wing intensities of the He II 304 Å line are low. Despite the fact that the line asymmetry increases with speed for both lines, it is more visible at low speeds (when the intensity in the wing is high enough). Finally, it is more pronounced at low temperatures because the scattering of the incident radiation is relatively more important as compared to collisional processes than it is at higher temperatures.

Figure 3 shows that the intensities of the Ca II lines are lower at 15 000 K than at 8000 K, an effect of Ca II to Ca III ionization (Gouttebroze & Heinzel 2002).

4. Diagnostics of Thermodynamic Parameters

We show here how the non-LTE radiative transfer calculations can help us to infer the thermodynamic properties of a prominence observed by the SUMER spectrometer on SOHO. This prominence was actually a rather quiet prominence and we have not included any velocity fields in these calculations. It was observed during the 13th MEDOC campaign held at IAS in June 2004. We select a few pixels in the SUMER slit which cut across the prominence and average the

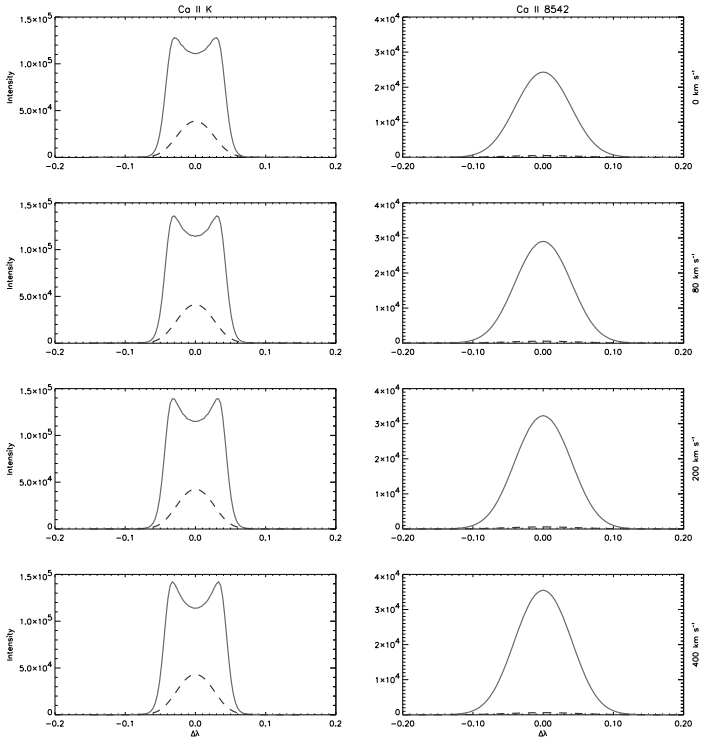

Figure 3. Same as in Fig. 2 for Ca II K and Ca II 8542 Å lines.

line profiles there. We consider the line profiles of two H resonance lines (Lyβ and Lyϵ) and the He I resonance line at 584 Å. For the comparison between computed and observed line profiles we now include the presence of a PCTR. The temperature variation between the cold prominence core and the corona suggested by Anzer & Heinzel (1999) has been adopted for this study. By a trial and error process we selected the temperature profile shown in Fig. 4. The other prominence parameters are $p = 0.023$ dyn cm^{-2}, $L = 194$ km (total column mass $2.4\,10^{-7}$ g cm^{-2}), $H = 113722$ km, and the microturbulent velocity $\xi = 18$ km s^{-1}.

We obtain a very good agreement between the computed profiles (convoluted with the SUMER instrumental profile) and the observed profiles, as shown in Fig. 5. It is worth noting that fitting hydrogen *and* helium resonance lines simultaneously places strong constraints on the parameter space, and it was not possible to find another set of parameters for the prominence that would be significantly different than what is given above and that would lead to a satisfactory fit of the observed profiles.

5. Conclusions

The non-LTE radiative transfer modeling that we are developing is a key tool for interpreting observations and constructing realistic prominence models. The combination of lines from hydrogen, helium, and calcium, places strong con-

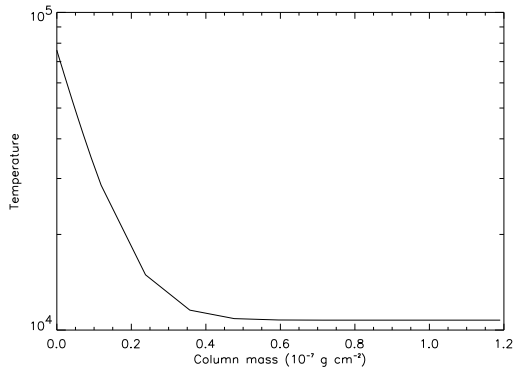

Figure 4. Temperature as a function of the column mass in one half of the prominence slab.

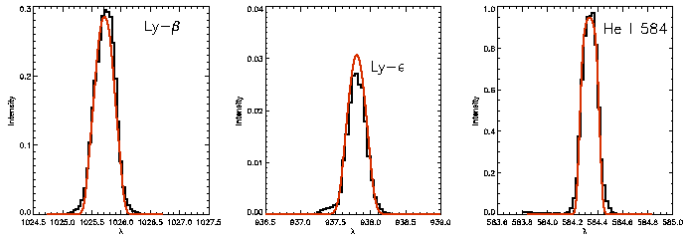

Figure 5. Observed (histograms) and computed (curves) lines profiles for Lyβ (left), Lyϵ (middle), and He I 584 Å (right).

straints on the models. Imaging and spectroscopy must be used for comparisons with calculations to determine thermodynamic parameters and velocities. The radial velocity determined from the comparison between observed and computed line profiles, in combination with line-of-sight velocities, should allow us to infer the full velocity vector of the prominence plasma. In a future work we will compare our model results with simultaneous observations of, e.g., Hα and He II 304 Å.

Acknowledgments. N. L. acknowledges financial support from the organisers of the Coimbra Solar Physics Meeting, the University of Wales through the Gooding Fund, and PPARC through grant PPA/G/O/2003/00017.

References

Anzer U., Heinzel P., 1999, A&A 349, 974
Gontikakis C., Vial J.-C., Gouttebroze P., 1997a, A&A 325, 803
Gontikakis C., Vial J.-C., Gouttebroze P., 1997b, Solar Phys. 172, 189
Gouttebroze P., Heinzel P., 2002, A&A 385, 273
Gouttebroze P., Labrosse N., 2000, Solar Phys. 196, 349
Heinzel P., Rompolt B., 1987, Solar Phys. 110, 171
Labrosse N., Gouttebroze P., 2001, A&A 380, 323
Labrosse N., Gouttebroze P., 2004, ApJ 617, 614

Labrosse N., Vial J. C., Gouttebroze P., 2006, Solar Active Regions and 3D Magnetic Structure, 26th IAU GA, JD 3, 47, 3